

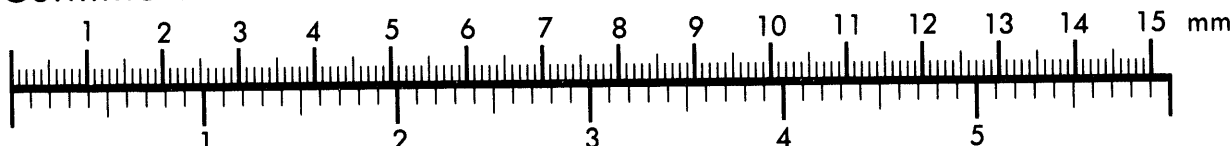


**AIIM**

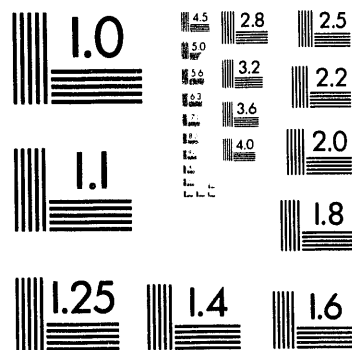
**Association for Information and Image Management**

1100 Wayne Avenue, Suite 1100  
Silver Spring, Maryland 20910  
301/587-8202

**Centimeter**



**Inches**



MANUFACTURED TO AIIM STANDARDS  
BY APPLIED IMAGE, INC.

1 of 1

## Pion Interferometry in $^{28}\text{Si} + \text{Pb}$ Central Collisions

Nu Xu

Department of Physics, SUNY Stony Brook, Stony Brook, New York 11794

For the E814 Collaboration: BNL, GSI, McGill Univ., Univ. of Pittsburg  
 SUNY Stony Brook, Univ. of São Paulo, Wayne State Univ., Yale Univ.

Two-pion correlation functions have been studied using the E814 apparatus in 14.6 A·GeV/c  $^{28}\text{Si} + \text{Pb}$  central collisions. Results of the correlation functions for pions from the RQMD event generator are compared to the data and show that a source with RMS radius of 8.3 fm is comparable with the experimental data.

### 1. INTRODUCTION

Quantum mechanics requires that the wave function of a bosonic system is symmetric under particle exchange. This leads to a quantum interference in the two-pion correlation function causing an enhancement at small relative momenta. The shape of the distribution near zero relative momentum is related to the size and the life-time [1,2] of the interaction region. In order to gain some insights into the collision dynamics, the correlation method has been used extensively in studies of relativistic heavy-ion collisions (see e.g., refs. [3,4]). In this paper, we report preliminary E814 pion interferometry results from central collisions ( $\sigma/\sigma_{\text{geom}} \leq 10\%$ ) between  $^{28}\text{Si}$  and Pb at a beam momentum of 14.6 A·GeV/c.

### 2. EXPERIMENTAL SETUP AND DATA

The E814 setup provides  $4\pi$  event characterization with a target calorimeter and a charged particle multiplicity detector. The forward spectrometer acceptance was determined by a lead collimator to  $-115 < \theta_x < 14$  mr (bending plane) and  $-21 < \theta_y < 21$  mr with respect to the beam direction. Particle identification is obtained by combination of time-of-flight and momentum measurement [5,6]. The acceptance in transverse momentum  $p_t$  and rapidity  $y$  of identified  $\pi^+$  and  $\pi^-$  is shown in Fig. 1. Note that pions of both charges are detected at  $p_t \geq 0$  with a mean rapidity of about 3.

The two-particle correlation function  $C_2$  is defined as:

$$C_2(q) = \frac{d^2N_{1,2}}{dp_1 dp_2} / \frac{dN_1}{dp_1} \frac{dN_2}{dp_2} \approx \frac{N_{tr}(q)}{N_{bk}(q)} \quad (1)$$

where  $q = \sqrt{-(p_1 - p_2)^2}$  is the relative 4-momentum between the two identical particles. As done frequently, the numerator  $N_{tr}(q)$  is obtained by taking particles from the same event, while the denominator  $N_{bk}(q)$  is constructed using two pions from different events (mixed event technique). This way one ensures that the statistical errors in the correlation function are determined by the statistics of the true pion pairs only.

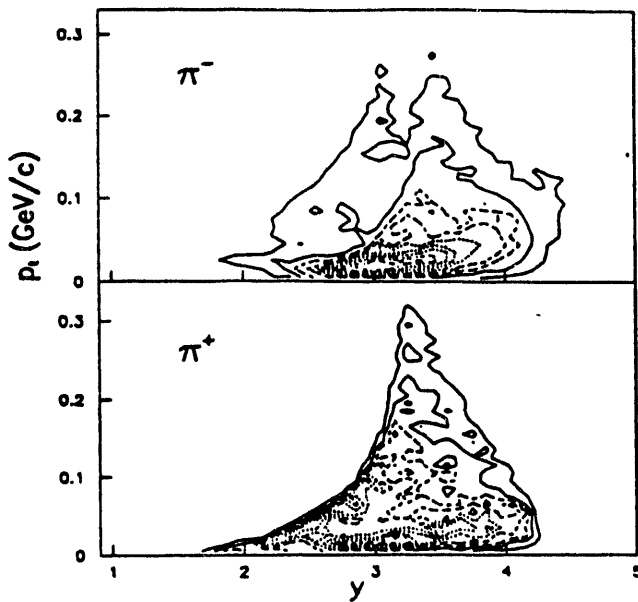


Figure 1. E814 acceptance.

The pion correlation functions corrected for Coulomb effects and two-particle acceptance are shown in Fig. 2 (open symbols). The total number of the selected  $\pi^-$ ( $\pi^+$ ) pairs is  $23.4k$ ( $4.3k$ ) and about 80% of the pairs are in the relative momentum range of  $0 \leq q \leq 0.3$  GeV/c. Error bars are statistical only. The background distribution is normalized to the total number of the entries in the true distributions within the range of  $0 \leq q \leq 1$  GeV/c. It can be seen from this figure that, for  $q \geq 0.1$  GeV/c, the distribution is consistent with unity. The Bose-Einstein enhancement is clear in the low relative momentum region for both like-sign pion pairs. Unlike-sign pion pairs (not shown here) show a ratio that is consistent with unity over the whole relative momentum range.

The measured correlation functions have been fitted by two commonly used parameterizations, namely, a Gaussian and an exponential function:

$$C_2^g(q) = 1 + \lambda \cdot \exp(-q^2 R^2); \quad C_2^e(q) = 1 + \lambda \cdot \exp(-qR). \quad (2)$$

where  $\lambda$  is the chaoticity parameter and  $R$  is the space-time extent of the pion source. The extracted fit parameters are summarized in Table 1. In Fig. 2 (left), the solid and dashed lines represent the Gaussian and exponential fits, respectively. While the reduced  $\chi^2$  is slightly smaller for the exponential fit, both functional forms are consistent with data. However, the source parameters are different by a large factor!

Table 1. Source parameters extracted from the Gaussian and exponential fits.

	$\pi^+$			$\pi^-$		
	$\lambda$	$R$ (fm)	$\chi^2/n$	$\lambda$	$R$ (fm)	$\chi^2/n$
Gauss	0.25(0.14)	3.4(1.2)	0.9	0.43(0.09)	4.4(0.6)	1.6
Exp.	0.41(0.27)	5.1(2.6)	0.7	0.81(0.19)	7.0(1.2)	1.4

Non-Gaussian shapes of the pion correlation functions have been observed in heavy-ion collisions as well as in hadron-hadron collisions [4,7,8]. The shape of correlation function, depends, besides the source distribution, on the experimental acceptance, resonance decays, and other effects. To overcome these ambiguities, rather than extracting the source size from fitting a certain functional form to the data, we use dynamical models with a known space-time characteristics of the source, impose the Bose-Einstein effect and evaluate the two particle correlation functions. In the next section, the RQMD model analysis is discussed.

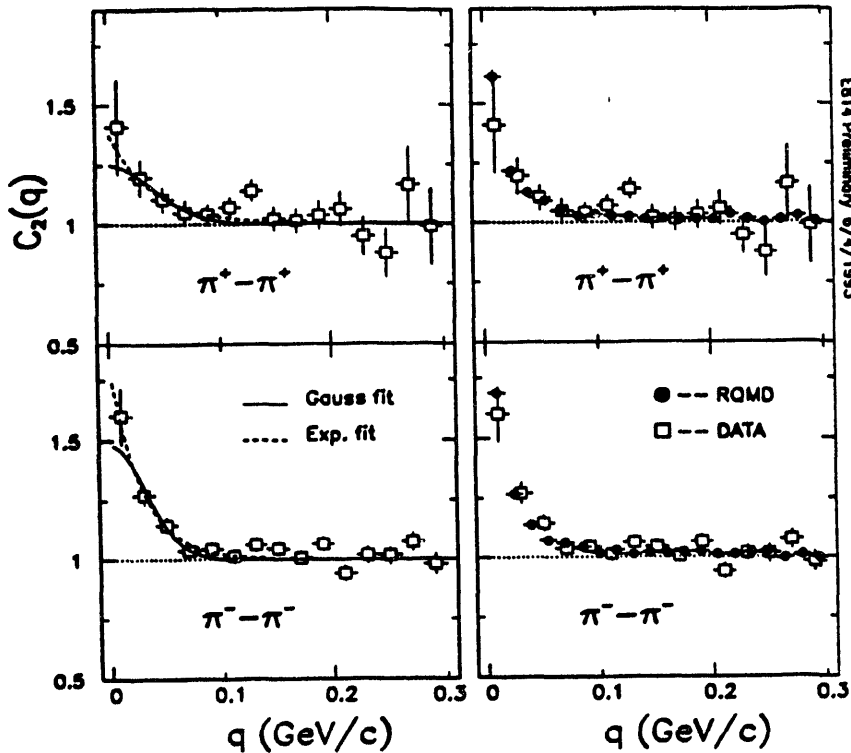


Figure 2. Pion correlation functions: (left) experimental data with Gaussian and exponential fits; (right) experimental data with RQMD results.

### 3. RQMD CALCULATIONS

The event generator RQMD [9] has been very successful in describing pion, proton, kaon, and other measured single-particle spectra [5,7,10] at both AGS and SPS energies. It is natural to use the model to also calculate the two-particle correlation functions.

Phase-space distributions from RQMD for a dimension  $x$  transverse to the beam direction are shown in Fig. 3 for  $14.6 \text{ A} \cdot \text{GeV}/c \text{ } ^{28}\text{Si} + \text{Pb}$  collisions at an impact parameter  $b = 1.0 \text{ fm}$ . These distributions were generated for pions at their freeze-out stage. The spatial distribution of pions into the E814 spectrometer acceptance is shown in hatched. Fig. 3 (left) indicates a clear correlation between momentum and spatial coordinates. An immediate consequence is that a spectrometer with finite  $p_t$  acceptance will not be able to 'see' particles emitted from all locations  $x$  of the source. Hence the extracted source size will be reduced. Indeed, with a  $p_t$  coverage not including the lowest  $p_t$ , our  $\pi^+$  correlation functions have shown a smaller size parameter [11] (2.2 vs. 3.4 fm). Such a  $p_t$ -dependence of the pion source size was also reported by Roland in this conference [12]. The origin of this dynamical correlation in RQMD is presumably due to pion absorption. But flow effects would also produce such a behavior. Qualitatively such a correlation is

also seen[13] in the event generator ARC.

In order to generate a two particle correlation function, the Koonin-Pratt method was used [14] to construct a symmetrized pion wave function from the RQMD generated single-particle distributions. The experimental conditions were imposed on the RQMD data before being fed into the calculation. Finally the correlation function was corrected by the Gamow factor as it has been done for experimental data. Results of the calculations, for both  $\pi^+$  and  $\pi^-$  within the E814 spectrometer, are shown in Fig. 2 (right). The agreement between the experiment and theory is excellent.

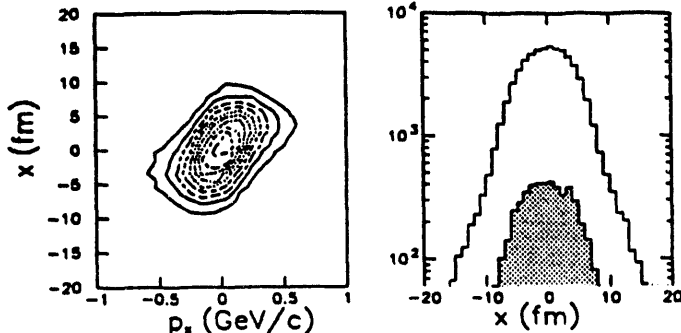


Figure 3. Phase-space distribution calculated from the RQMD event generator. (left) Contour plot of the position vs. momentum distribution in  $x$ -direction; (right)  $x$ -position distribution. The hatched region represents the distribution within the E814 acceptance.

The fact that the RQMD model can reproduce experimental single-particle spectra and two-pion correlation functions suggests that its phase-space distributions correctly represent the collision dynamics at the AGS energies. Our results demonstrate that, for  $^{28}\text{Si} + \text{Pb}$  central collisions, the spatial extent of the source (in the center of mass frame) of  $R_x = 4.71$ ,  $R_y = 4.75$ ,  $R_z = 4.91$  fm as produced by RQMD is consistent with our data. The corresponding effective RMS pion source size is 8.3 fm, implying an expansion in transverse radius by a factor of 2.3 between the early stage of the collision and freeze-out.

#### ACKNOWLEDGEMENTS

The author is indebted to Drs. S. Pratt and H. Sorge for valuable discussions and their kindness to provide computer codes. We are grateful for support received from the U.S. DOE, U.S. NSF, Canadian NSERC, and CNPq Brazil.

#### REFERENCES

1. G. Goldhaber, S. Goldhaber, W. Lee, and A. Pais, Phys. Rev. **120**, 300(1960).
2. E.V. Shuryak, Phys. Lett. **B44**, 387(1973).
3. T. Abbott, *et al.*, E802 Collaboration, Phys. Rev. Lett. **69**, 1030(1992).
4. A. Bamberger, *et al.*, NA35 Collaboration, Phys. Lett. **B203**, 320(1988).
5. J. Barrette, *et al.*, E814 Collaboration, Z. Phys., **C59**, (1993).
6. P. Braun-Munzinger *et al.*, E814 Collaboration, Nucl. Phys. **A544**, 137c(1991).
7. J.P. Sullivan, *et al.*, Phys. Rev. Lett., **70**, 3000(1993).
8. T. Åkesson, *et al.*, AFS Collaboration, Z. Phys. **C36**, 517(1987).
9. H. Sorge, H. Stöcker, and W. Greiner, Nucl. Phys. **A498**, 567c(1989).
10. Th. Schönfeld, *et al.*, Nucl. Phys. **A544**, 439c(1991).
11. N. Xu, E814 Collaboration, Proceedings of HIPAGS'93, MIT LNS-2158, p.362.
12. G. Roland, NA35 Collaboration, these Proceedings.
13. O. Vossack, E802 Collaboration, Proceedings of HIPAGS'93 Workshop, MIT LNS-2158, p.380.
14. S. Pratt, Phys. Rev. Lett. **53**, 1219(1984); S. Pratt, Phys. Rev. **D33**, 72(1986); S. Pratt, *et al.*, Phys. Rev. **C42**, 2646(1990).

## **DISCLAIMER**

This report was prepared as an account of work sponsored by an agency of the United States Government. Neither the United States Government nor any agency thereof, nor any of their employees, makes any warranty, express or implied, or assumes any legal liability or responsibility for the accuracy, completeness, or usefulness of any information, apparatus, product, or process disclosed, or represents that its use would not infringe privately owned rights. Reference herein to any specific commercial product, process, or service by trade name, trademark, manufacturer, or otherwise does not necessarily constitute or imply its endorsement, recommendation, or favoring by the United States Government or any agency thereof. The views and opinions of authors expressed herein do not necessarily state or reflect those of the United States Government or any agency thereof.

**DATE  
FILMED**

**8/25/94**

**END**

